

Communication

# Extracellular Heat Shock Protein 27 Is Released by Plasma-Treated Ovarian Cancer Cells and Affects THP-1 Monocyte Activity

Debora Singer <sup>1</sup>, Can Pascal Wulff <sup>1,2</sup>, Matthias B. Stope <sup>3</sup> and Sander Bekeschus <sup>1,\*</sup>

<sup>1</sup> ZIK *plasmatis*, Leibniz Institute for Plasma Science and Technology (INP), Felix-Hausdorff-Str. 2, 17489 Greifswald, Germany

<sup>2</sup> Clinic and Policlinic for Urology, Greifswald University Medical Center, Ferdinand-Sauerbruch-Str., 17475 Greifswald, Germany

<sup>3</sup> Department of Gynecology and Gynecological Oncology, Bonn University Medical Center, 53127 Bonn, Germany

\* Correspondence: sander.bekeschus@inp-greifswald.de

**Abstract:** Heat shock protein 27 (Hsp27) is a cytoprotective molecule and is inducible via oxidative stress. Anti-cancer therapies, such as the recently investigated gas plasma, subject tumor cells to a plethora of reactive oxygen species (ROS). In ovarian tumor microenvironments (TME), immune cells such as monocytes and macrophages can be found in large numbers and are often associated with cancer progression. Therefore, we quantified extracellular Hsp27 of OVCAR-3 and SK-OV-3 cells after gas plasma exposure in vitro. We found Hsp27 to be significantly increased. Following this, we investigated the effects of Hsp27 on THP-1 monocytes. Live cell imaging of Hsp27-treated THP-1 cells showed decelerated cell numbers and a reduction in cell cluster sizes. In addition, reduced metabolic activity and proliferation were identified using flow cytometry. Mitochondrial ROS production decreased. Using multicolor flow cytometry, the expression profile of eight out of twelve investigated cell surface markers was significantly modulated in Hsp27-treated THP-1 cells. A significantly decreased release of IL18 accommodated this. Taken together, our results suggest an immunomodulatory effect of Hsp27 on THP-1 monocytes. These data call for further investigations on Hsp27's impact on the interplay of ovarian cancer cells and monocytes/macrophages under oxidative stress conditions.

**Keywords:** gas plasma; Hsp27; oxidative stress; reactive oxygen species; ROS



**Citation:** Singer, D.; Wulff, C.P.; Stope, M.B.; Bekeschus, S.

Extracellular Heat Shock Protein 27 Is Released by Plasma-Treated Ovarian Cancer Cells and Affects THP-1 Monocyte Activity. *Plasma* **2022**, *5*, 569–578. <https://doi.org/10.3390/plasma5040040>

Academic Editor: Emilio Martines

Received: 8 November 2022

Accepted: 2 December 2022

Published: 6 December 2022

**Publisher's Note:** MDPI stays neutral with regard to jurisdictional claims in published maps and institutional affiliations.



**Copyright:** © 2022 by the authors. Licensee MDPI, Basel, Switzerland. This article is an open access article distributed under the terms and conditions of the Creative Commons Attribution (CC BY) license (<https://creativecommons.org/licenses/by/4.0/>).

## 1. Introduction

The heat shock protein 27 (Hsp27) is one of the major molecules induced in response to several stress conditions, such as oxidative stress [1,2]. Oxidative stress can be triggered via increased levels of reactive oxygen species (ROS), which damage the cell by direct oxidation of biomolecules or disruption of the redox signaling [3]. The protective effect of Hsp27 is mediated by its ability to inhibit caspase activation [4]. In addition, it can promote proteasomal degradation of oxidized proteins [5] and regulate the actin cytoskeleton and its antioxidant function [6–8].

In cancer therapy, however, the cytotoxic effects of ROS are also exploited. This is apparent in several types of chemotherapy [9] and photodynamic therapy [10]. In addition, a relatively recent approach dwelling on medical gas plasma technology is being explored [11]. In gas plasma-treated tumor cells, cytotoxic effects were demonstrated for several cancer entities, such as head and neck [12–14], leukemia [15–17], prostate [18–20], and ovarian [21–23] cancer. Epithelial ovarian cancer ranks seventh among cancers diagnosed in women in 2018, being the most lethal gynecological cancer with a 5-year survival rate of only 46% after diagnosis [24]. This calls for a better understanding of these tumor cells and therapeutic modalities.

The tumor microenvironment (TME) in ovarian cancer is infiltrated by immune cells, such as monocytes, that later differentiate into macrophages [25,26]. Often, those macrophages are so-called tumor-associated macrophages (TAMs) [27]. TAMs are related to tumor progression and metastasis [28,29]. This highlights the necessity to investigate the effects of possible cancer therapies not only on tumor cells but also on monocytes/macrophages, which interact in the TME. In this study, we found significantly increased Hsp27 release in plasma-treated ovarian cancer cells. To explore the potential effects on immune cells present in the TME, we aimed to investigate the effects of Hsp27 on THP-1 monocytes.

## 2. Materials and Methods

### 2.1. Cell Culture

The myeloid cell line used in this study was THP-1 (ATCC: TIB-202). The two ovarian cancer cell lines were OVCAR-3 (ATCC: HTB-161) and SK-OV-3 (ATCC: HTB-77). The cells were cultured using Roswell Park Memorial Institute (RPMI) 1640 Medium. Fetal bovine serum (10%), L-glutamine (2%), and penicillin/streptomycin (1% each) were added to supplement the cell culture medium (all Sigma-Aldrich, Taufkirchen, Germany). The cells were cultured under standard conditions (37 °C, 5% CO<sub>2</sub>, and 95% humidity) as described before [30]. The growth parameters of two ovarian cancer cell lines were outlined in detail previously [22].

### 2.2. Gas Plasma Treatment

For the gas plasma treatment,  $2 \times 10^5$  ovarian cancer cells in 500 µL of fully supplemented cell culture medium were seeded to 24-well plates (NUNC, Roskilde, Denmark). Next, while still in suspension, they were exposed for 30 s to the ROS produced by the atmospheric pressure plasma jet kINPen (neoplas med, Greifswald, Germany). The device's frequency was 1 MHz, and the dissipated power was approximately 1 W [31]. The distance from the jet's nozzle to the liquid surface was 20 mm. The jet was operated with argon (Air Liquide, Bremen, Germany) as feed gas at a total flux of four standard liters per minute. In control conditions, cells were exposed to argon gas alone, without the plasma ignition. For maximum precision of parameter control, the gas plasma jet was mounted to an *xyz*-stage (CNC, Hamburg, Germany) and computer-controlled to hover over the center of each well for the indicated time. More details on the general treatment procedure have been described before [30].

### 2.3. Hsp27 Quantification

Twenty-four hours after gas plasma treatment of ovarian cancer cells, cell culture supernatants were collected and stored for subsequent enzyme-linked immunosorbent assays (ELISA). Heat shock protein 27 (Hsp27) concentration was measured using the Human Hsp27 DuoSet ELISA kit (catalog number: DY1580; RnD Systems, Wiesbaden, Germany) according to the manufacturer's protocol. Briefly, a 96-well plate was coated with a capture antibody capable of binding Hsp27. Then, cell culture supernatants were added and incubated. After washing three times with PBS, the plates were incubated with a biotinylated detection antibody labeled with streptavidin conjugated to horseradish peroxidase. The HRP substrate solution was added for 20 min. The reaction was stopped with a stopping solution. The resulting optical density was measured at 450 nm using a microplate reader (Infinite M200; Tecan, Männedorf, Switzerland). The Hsp27 concentrations were calculated against a known standard dilution of recombinant human Hsp27.

### 2.4. Live-Cell High-Content Imaging

The high-content imaging device Operetta confocal laser scanning (CLS) (PerkinElmer, Hamburg, Germany) was pre-heated to 37 °C and set to 5% CO<sub>2</sub> to enable live-cell imaging. Images were acquired six days after treatment with 1 ng/mL Hsp27 (Enzo Life Sciences, Lörrach, Germany). A 20× air objective (NA 0.4; Zeiss, Jena, Germany) was utilized for

image acquisition. Brightfield and digital phase contrasts were employed as acquisition channels, as described before [30]. Multiple fields of view were acquired per well.

### 2.5. Metabolic Activity and Viability

The resazurin-based assay was used to determine the THP-1 cells' metabolic activity, as described before [32]. Briefly, 24 h after Hsp27 treatment (1 ng/mL), a final concentration of 100  $\mu$ M resazurin was added to the cells and incubated for 4 h. Metabolically active cells reduce resazurin to resorufin [33], which was quantified by measuring its fluorescence using a microplate reader (Infinite F200; Tecan) at  $\lambda_{\text{ex}}$  535 nm and  $\lambda_{\text{em}}$  590 nm. Viability analysis of THP-1 cells after Hsp27 addition was performed by live/dead cell discrimination using 4',6-diamidino-2-phenylindole (DAPI, 1  $\mu$ M; BioLegend, Amsterdam, The Netherlands) staining and fluorescence analysis using flow cytometry (CytoFLEX S; Beckman-Coulter, Krefeld, Germany).

### 2.6. Analysis of Oxidation and Mitochondria

Intracellular ROS generation was assessed by staining the myeloid cells either with chloromethyl 2',7'-dichlorodihydrofluorescein diacetate (CM-H<sub>2</sub>DCF-DA, 1  $\mu$ M; Thermo Fisher Scientific, Dreieich, Germany) or hydroxyphenyl fluorescein (HPF, 1  $\mu$ M; Thermo Fisher Scientific), as described before [34]. Briefly,  $2 \times 10^4$  stained cells were seeded into 96-well plates and subsequently exposed to Hsp27. To determine the mitochondrial membrane potential, the myeloid cells were stained with mitotracker orange (MTO, 1  $\mu$ M; Thermo Fisher Scientific) before adding Hsp27. In all three assays, DAPI was used to discriminate viable from dead cells. The mean fluorescence intensity (MFI) of all three dyes was analyzed using flow cytometry. In addition, the ROS were quantified in supernatants collected immediately after gas plasma treatment of ovarian cancer cells. For this, the Amplex Ultrared Assay (Thermo Fisher Scientific) was used, as previously described [30].

### 2.7. Cell Surface Marker Expression Analysis

Multicolor flow cytometry was performed to analyze the expression of the following surface markers on THP-1 cells: cluster of differentiation (CD)15, CD33, CD41, CD45RA, CD49d, CD55, CD63, CD66b, CD69, CD154, CD271, and human leukocyte antigen HLA-ABC. Cells were harvested 144 h after treatment, transferred to 96-well V-bottom plates, washed, and stained with fluorescently labeled monoclonal antibodies. DAPI was added to determine live-cell populations only. The samples were incubated for 15 min at 20 °C in the dark. Then, the cells were washed and fluorescence intensities were assessed using flow cytometry (CytoFLEX S; Beckman-Coulter).

### 2.8. Cytokine Quantification

A bead-based assay (LEGENDplex; BioLegend) was used to quantify the following 13 cytokines: interferon (IFN-) $\alpha$ , IFN- $\gamma$ , interleukin (IL)1 $\beta$ , IL6, IL8, IL10, IL12p70, IL17A, IL18, IL23, IL33, monocyte chemoattractant protein 1 (MCP1), and tumor necrosis factor (TNF) $\alpha$ . Cell culture supernatants were collected 144 h after the addition of Hsp27. The assay was performed according to the manufacturer's protocol and measured using flow cytometry, as described before [35]. Calculation against a known standard was performed using a 5-log fitting.

### 2.9. Statistical Analysis and Software

Prism 9.4.1 (Graphpad Software, San Diego, CA, USA) was used to perform statistical analysis. One-way analysis of variances (ANOVA) or an unpaired two-tailed *t*-test was applied to statistically compare treated against control groups. The level of significance is indicated as follows:  $p < 0.05$  (\*),  $p < 0.01$  (\*\*), and  $p < 0.001$  (\*\*\*). Kaluza analysis 2.1.1 software (Beckman-Coulter) was used to analyze flow cytometry data. Cytokine data were analyzed with LEGENDplex software (BioLegend). High-content image analysis was performed using Harmony 4.9 (PerkinElmer) software.

### 3. Results

#### 3.1. Hsp27 Release Was Induced upon Gas Plasma Treatment in Ovarian Cancer Cells

OVCAR-3 and SK-OV-3 cells were treated with an argon plasma jet and the release of Hsp27 was quantified (Figure 1a). The plasma treatment led to a significant increase in extracellular Hsp27 concentrations in both ovarian cancer cell lines compared to untreated cells. Gas plasma generates ROS. High ROS concentrations lead to oxidative stress and Hsp27 release. To causatively link the ROS deposition to Hsp27 release, the ROS were quantified in cell culture supernatants collected immediately after gas plasma exposure. Extracellular ROS increased in a plasma treatment time-dependent manner (Figure A1). At 30 s treatment times, SK-OV-3 cells showed significantly lower extracellular ROS levels compared to OVCAR-3 cells. This suggested the former has a larger antioxidative capacity than the latter. Whether this was causative to the relatively lower Hsp27 release of SK-OV-3 cells was beyond the scope of this study. Next, to understand the changes Hsp27 could induce in human immune cells, THP-1 monocytes were incubated with this heat shock protein. Several types of analysis were conducted. First, live-cell imaging was performed 144 h after exposure of the THP-1 cells to Hsp27 (Figure 1b). In microscopy, it appeared that the Hsp27-treated THP-1 cells tended to form fewer large aggregates compared to their vehicle counterparts. Subsequently, algorithm-based quantitative image analysis of such THP-1 clusters and other morphological features revealed significant changes compared to their vehicle controls (Figure 1c). The number of cells forming clusters decreased modestly. At the same time, the number of single cells (not located in clusters) decreased significantly. However, the ratio between cluster and single cells remained unchanged. The area of clusters also decreased significantly upon Hsp27 treatment. These findings suggested a different behavior of THP-1 monocytes in the presence of Hsp27. A principal component analysis (PCA) across the multiple morphological image parameter features that was calculated revealed that Hsp27-treated cells differed from vehicle controls for three independent biological replicates (Figure 1d). Therefore, further analyses were performed to identify the putative effects of extracellular Hsp27 on THP-1 monocytes (Figure 1e).

#### 3.2. Extracellular Hsp27 Affected THP-1 Metabolic Activity and Proliferation

To investigate if Hsp27 affected THP-1 cells' metabolic activity, resazurin assays were performed. Metabolically active cells transform non-fluorescent resazurin (blue) to fluorescent resorufin (pink) (Figure 2a). Compared to the control, a significant decrease of approximately 15% was found in response to Hsp27 addition in THP-1 monocytes (Figure 2b). This indicated that the cells not only had changed based on morphological features but also regarding cellular metabolism. Furthermore, the THP-1 cells' viability was analyzed using DAPI staining and flow cytometry (Figure 2c). A modest but significant decrease was found (Figure 2d). This suggested that Hsp27 was anti-proliferative to some THP-1 monocytes while overall changing their metabolic activity and morphology. In addition, the THP-1 cell counts were significantly reduced (Figure 2e). We next assessed whether the Hsp27 addition to THP-1 monocytes acutely changed their intracellular oxidative milieu. To this end, the cytosolic fluorescent redox-sensitive dyes DCF and HPF, as well as the mitochondrial membrane potential-dependent dye MTO (Figure 2f), were used. Cytosolic ROS or antioxidants were affected by Hsp27 addition, as unchanged DCF and HPF fluorescence suggested (Figure 2g). By contrast, MTO was significantly decreased upon Hsp27 addition to the THP-1 cells. As mitochondria are the powerhouse of cells to generate energy for metabolic activity, the cell's metabolic activity decline (Figure 2b), and mitochondrial membrane potential reduction (Figure 2g) may be linked.

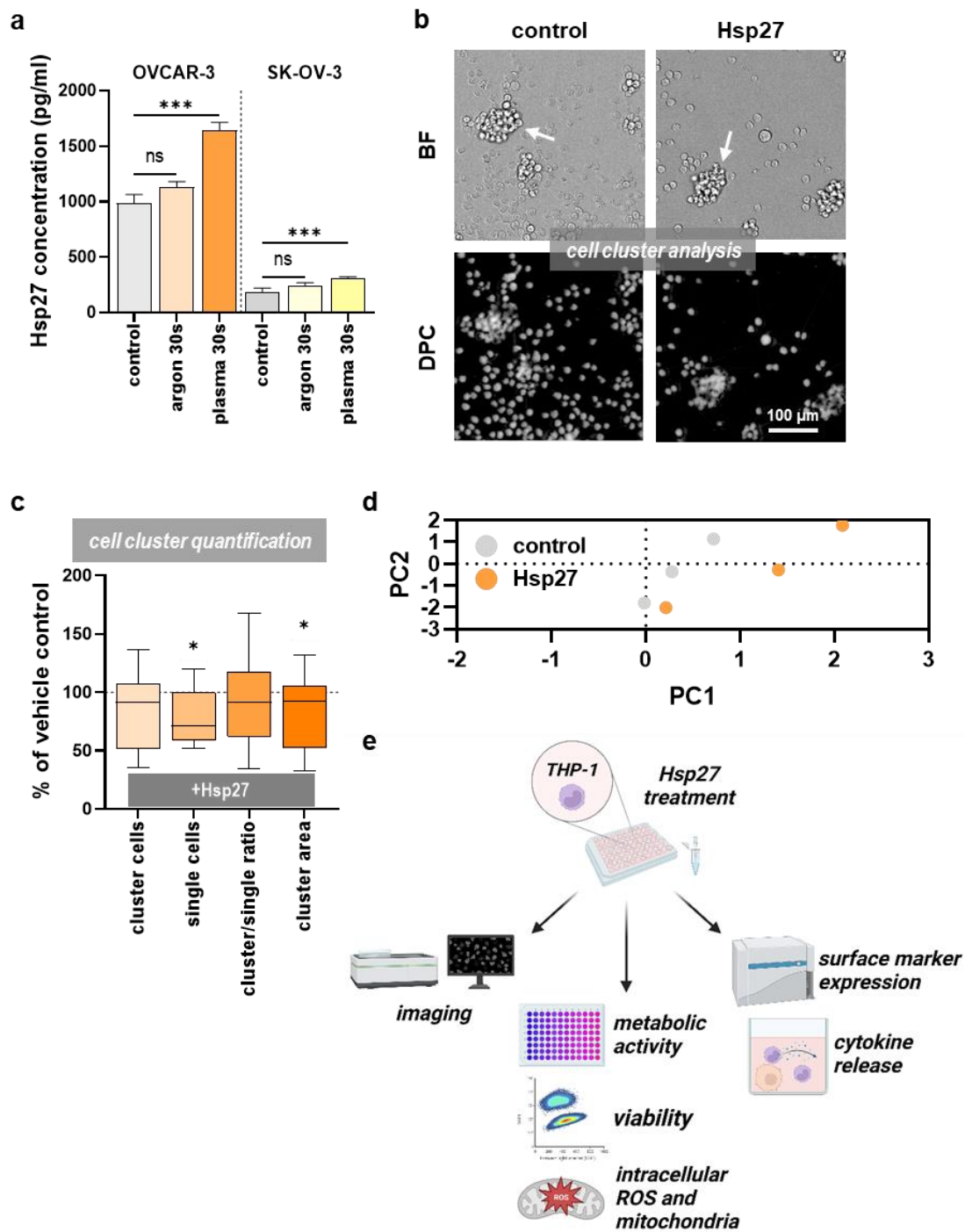


**Figure 1.** Hsp27 release in ovarian cancer cells and effects on the THP-1 cells. (a) Hsp27 release 24 h after 30 s argon plasma treatment in OVCAR-3 and SK-OV-3 cells; (b) representative images of untreated (control) and Hsp27-incubated THP-1 cells captured in the brightfield (BF) and digital phase contrast (DPC) channel 144 h after treatment; clusters are indicated with white arrows; (c) algorithm-based quantification of THP-1 cell cluster properties 144 h after addition of Hsp27 compared to the vehicle-treated (solvent control) cells for the parameter’s cluster cells, single cells, cluster over single cell ratio, and total cluster cell area, showing a significant decrease in the second and fourth metric caused by Hsp27; (d) principal component analysis of vehicle (grey) and Hsp27 (orange) treated THP-1 cells taking into account multiple morphological features as extracted using Harmony quantitative imaging software; (e) study-protocol of further Hsp27 exposure to the THP-1 cells. Statistical analysis was performed using one-way ANOVA (a) or using an unpaired two-tailed *t*-test (c) with  $p < 0.05$  (\*) and  $p < 0.001$  (\*\*). ns = not significant. Scale bar is 100  $\mu$ m (b).

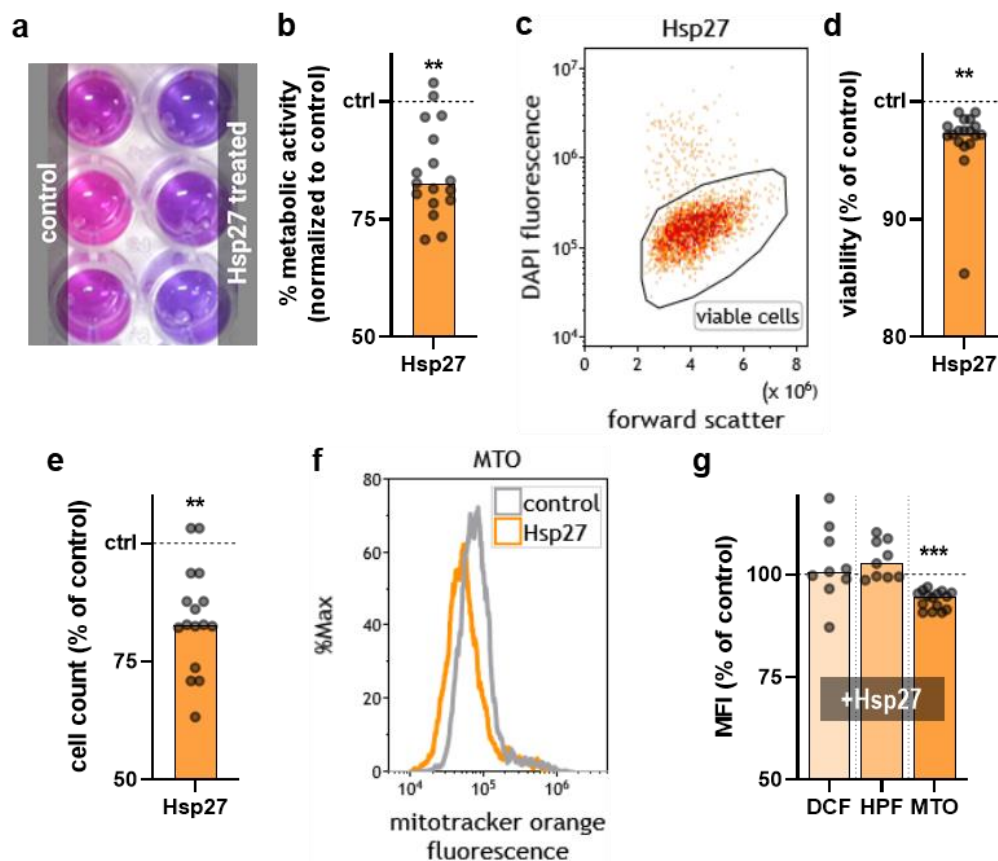


**Figure 2.** THP-1 metabolic activity, viability, and oxidation processes upon Hsp27 exposure. (a) representative photograph of the resazurin-based metabolic activity assay in the control and Hsp27-treated THP-1 cells; (b) normalized metabolic activity of the THP-1 cells 24 h after Hsp27 exposure; (c) representative flow cytometry dot plot of the Hsp27-treated THP-1 cells; (d,e) normalized viability (d) and cell counts (e) of the THP-1 cells 24 h after Hsp27 exposure; (f) representative flow cytometry overlay histograms of mitotracker orange fluorescence in the THP-1 cells in the presence or absence of extracellular Hsp27; (g) normalized (vehicle) mean fluorescence intensity (MFI) of DCF, APF, and MTO-stained and Hsp27-treated THP-1 cells. Statistical analysis was performed using an unpaired two-tailed *t*-test with  $p < 0.01$  (\*\*) and  $p < 0.001$  (\*\*\*).

### 3.3. Extracellular Hsp27 Affected the THP-1 Surface Marker Profile and IL18 Release

To investigate whether Hsp27 addition altered the THP-1 monocyte surface marker expression, twelve surface markers were analyzed 144 h after treatment using multicolor flow cytometry (Figure 3a). Out of these, CD15, CD55, and CD63 were modestly but significantly increased (Figure 3b). The strongest and most consistent significant increase upon Hsp27 exposure was found for CD33, CD41, and CD66b. By contrast, CD49d and HLA-ABC expression decreased modestly but significantly in Hsp27-treated monocytes. Next, the release of 13 cytokines after 144 h was also investigated. Only two analytes (MCP1, IL18) were above the detection limit (Table 1). Of those two, MCP-1 secretion of the THP-1 cells was significantly decreased after Hsp27 treatment. These data suggest that Hsp27 addition has immunomodulatory properties, as indicated by an altered surface marker profile and decreased IL18 release.

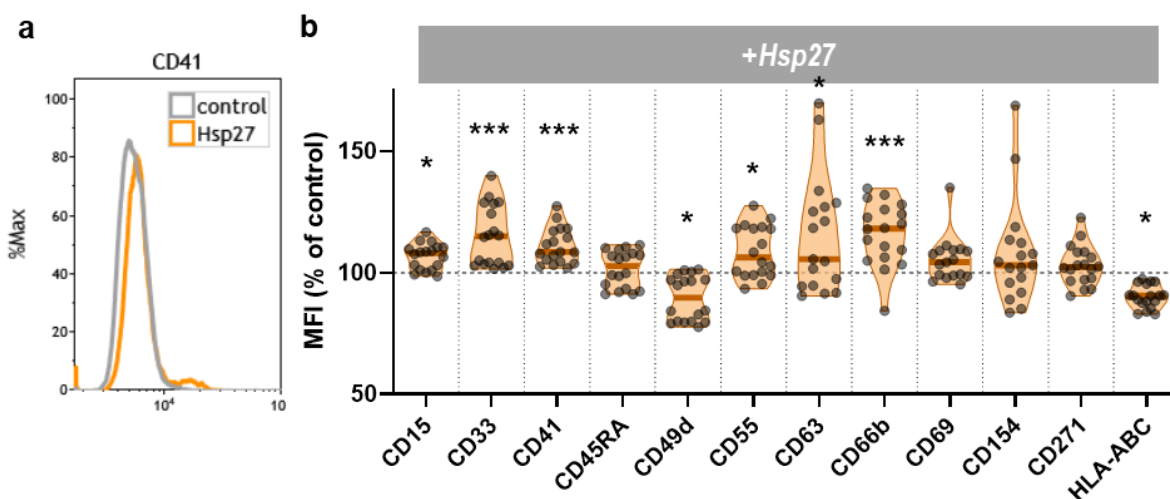


**Figure 3. THP-1 surface marker expression.** (a) representative flow cytometry overlay histograms of CD41 fluorescence in THP-1 cells cultured in the presence or absence of Hsp27; (b) normalized mean fluorescence intensity (MFI) of twelve surface markers of the THP-1 cells 144 h after Hsp27 exposure. Statistical analysis was performed using an unpaired two-tailed *t*-test with  $p < 0.05$  (\*) and  $p < 0.001$  (\*\*\*)

**Table 1. Multiplex chemokine and cytokine measurement.** The THP-1 cells were incubated in the presence or absence of Hsp27 and supernatants were collected 144 h later for multiplex chemokine and cytokine analysis performed using flow cytometry. Most analytes were below the detection limit (indicated by “<”); IL18 differed significantly (bold), as tested using a *t*-test. Concentrations are given in pg/mL.

|         | IFN $\alpha$ | IFN $\gamma$ | IL1 $\beta$ | IL6   | IL8   | IL10  | IL12p70 | IL17A | IL18        | IL23  | IL33  | TNF $\alpha$ | MCP1  |
|---------|--------------|--------------|-------------|-------|-------|-------|---------|-------|-------------|-------|-------|--------------|-------|
| Vehicle | <0.72        | <2.67        | <2.48       | <2.35 | <2.12 | <1.15 | <1.27   | <4.16 | <b>3.45</b> | <3.40 | <2.96 | <1.73        | 12.17 |
| Hsp27   | <0.72        | <2.67        | <2.48       | <2.35 | <2.12 | <1.15 | <1.27   | <4.16 | <b>1.64</b> | <3.40 | <2.96 | <1.73        | 10.06 |

#### 4. Discussion

In the present study, we investigated the effects of extracellular Hsp27 on THP-1 monocytes. Compared to untreated cells, Hsp27 caused inhibiting effects on the monocytes’ metabolic activity and proliferation and induced changes in their activation marker profile.

In our study, argon gas plasma treatment of ovarian cancer cell lines led to an enhanced release of Hsp27. This was expected since the main effects of gas plasma treatment are mediated by various ROS submitted to the cells, generating oxidative stress conditions [36,37]. Oxidative stress typically increases Hsp27 production and mediates cytoprotective mechanisms [5]. Secretion of Hsp27 has already been shown in ovarian cancer cells [38] and is associated with elevated metastasis [39], but less is known about the effects on the TME and its cells mediated by the extracellular Hsp27. Since monocytes and macrophages in ovarian cancer TME are also associated with metastasis [32,33], extracellular Hsp27 on monocytes was further investigated.

The growth of the THP-1 cells was inhibited by extracellular Hsp27, as visible from the reduced size of cell clusters and reduced cell count in general. These findings prompted us to perform a surface marker investigation, as differences in monocyte cell cluster formation were recently attributed to changes in maturation and differentiation [40]. In addition, metabolic activity was reduced, but not viability. This underlines that Hsp27 inhibited or prolonged THP-1 cell proliferation quite a bit. Regarding the oxidative milieu inside the THP-1 cells, we found Hsp27 to reduce mitochondrial ROS significantly. This indicates that extracellular Hsp27 could also have antioxidative properties as it is known for its intracellularly expressed protein [41].

Finally, the expression levels of monocyte activation markers were investigated, showing eight significant changes. Interestingly, CD41, also known as integrin alpha-2b [42], and CD66b [43], both played roles in the cell adhesion processes, increasing upon Hsp27 treatment. CD41 has been reported to respond to activation stimuli in THP-1 cells [44]. CD33, in turn, is a marker of immunosuppressive myeloid-derived suppressor cells (MDSCs) [45]. Nevertheless, the changes were modest, indicating a tendency towards activating the THP-1 cells but no full differentiation of the monocytes. This corroborates the finding that extracellular Hsp27 can mediate immunomodulation by balancing pro- and anti-inflammatory effects in THP-1 monocytes [46].

In summary, our findings show modest effects on THP-1 monocytes when exposed to a physiological concentration—relevant in the gas plasma treatment of ovarian cancer cells—of extracellular Hsp27. We found those effects to be characterized as anti-proliferative and immunomodulatory. More detailed analysis of how extracellular Hsp27 in the tumor environment might benefit the cancer cells by inhibiting macrophages in the TME is needed using complex models, such as in vivo studies. In addition, the impact of Hsp27 on differentiation towards potential TAM differentiation needs to be further studied in future work together with other immune cell types found in ovarian cancer TME.

**Author Contributions:** Conceptualization, M.B.S. and S.B.; methodology, S.B.; software, S.B.; validation, D.S. and C.P.W.; formal analysis, D.S. and C.P.W.; investigation, C.P.W.; resources, S.B.; data curation, D.S.; writing—original draft preparation, D.S. and S.B.; supervision, M.B.S. and S.B.; project administration, S.B.; funding acquisition, S.B. All authors have read and agreed to the published version of the manuscript.

**Funding:** This work was supported by the German Federal Ministry of Education and Research (BMBF) granted to SB, grant numbers 03Z22DN11 and 03Z22Di1.

**Institutional Review Board Statement:** Not applicable.

**Informed consent statement:** Not applicable.

**Data Availability Statement:** The data can be retrieved from the corresponding author upon reasonable request.

**Acknowledgments:** The authors acknowledge technical support by Felix Niessner.

**Conflicts of Interest:** The authors declare no conflict of interest.

## Appendix A

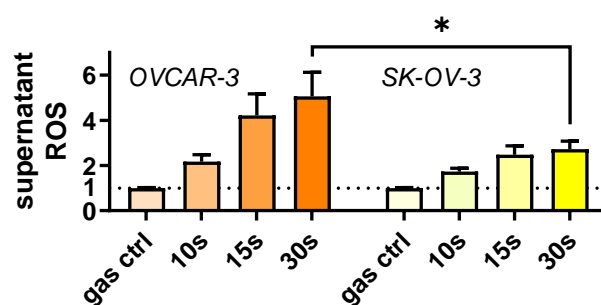


**Figure A1. Ovarian cancer supernatant ROS.** Ovarian cancer cells were gas plasma-treated for different treatment times (or exposed to argon gas only for 30 s = gas ctrl). Supernatant ROS ( $H_2O_2$ ) were quantified immediately after using Amplex UltraRed and normalized to gas control values. Data are mean +SEM eight replicates. Statistical analysis was performed using a one-way analysis of variances with  $p < 0.05$  (\*).

## References

1. Kim, J.; Lim, H.; Kim, S.; Cho, H.; Kim, Y.; Li, X.; Choi, H.; Kim, O. Effects of HSP27 downregulation on PDT resistance through PDT-induced autophagy in head and neck cancer cells. *Oncol. Rep.* **2016**, *35*, 2237–2245. [[CrossRef](#)] [[PubMed](#)]
2. Ikwegbue, P.C.; Masamba, P.; Oyinloye, B.E.; Kappo, A.P. Roles of Heat Shock Proteins in Apoptosis, Oxidative Stress, Human Inflammatory Diseases, and Cancer. *Pharmaceuticals* **2017**, *11*, 2. [[CrossRef](#)] [[PubMed](#)]
3. Sies, H.; Berndt, C.; Jones, D.P. Oxidative Stress. *Annu. Rev. Biochem.* **2017**, *86*, 715–748. [[CrossRef](#)] [[PubMed](#)]
4. Garrido, C.; Bruey, J.M.; Fromentin, A.; Hammann, A.; Arrigo, A.P.; Solary, E. HSP27 Inhibits Cytochrome c-Dependent Activation of Procaspase-9. *FASEB J.* **1999**, *13*, 2061–2070. [[CrossRef](#)]
5. Arrigo, A.-P. HSP27: Novel regulator of intracellular redox state. *IUBMB Life* **2001**, *52*, 303–307. [[CrossRef](#)] [[PubMed](#)]
6. Vidyasagar, A.; A Wilson, N.; Djamali, A. Heat shock protein 27 (HSP27): Biomarker of disease and therapeutic target. *Fibrogenesis Tissue Repair* **2012**, *5*, 7. [[CrossRef](#)]
7. Mehlen, P.; Kretz-Remy, C.; Préville, X.; Arrigo, A.P. Human Hsp27, Drosophila Hsp27 and Human Alpha-Crystallin Expression-Mediated Increase in Glutathione Is Essential for the Protective Activity of These Proteins against Tnfalpha-Induced Cell Death. *EMBO J.* **1996**, *15*, 2695–2706. [[CrossRef](#)]
8. Arrigo, A.-P.; Viot, S.; Chaufour, S.; Firdaus, W.; Kretz-Remy, C.; Diaz-Latoud, C. Hsp27 Consolidates Intracellular Redox Homeostasis by Upholding Glutathione in Its Reduced Form and by Decreasing Iron Intracellular Levels. *Antioxidants Redox Signal.* **2005**, *7*, 414–422. [[CrossRef](#)]
9. Yang, H.; Villani, R.M.; Wang, H.; Simpson, M.J.; Roberts, M.S.; Tang, M.; Liang, X. The role of cellular reactive oxygen species in cancer chemotherapy. *J. Exp. Clin. Cancer Res.* **2018**, *37*, 266. [[CrossRef](#)]
10. Dąbrowski, J.M. Chapter Nine—Reactive Oxygen Species in Photodynamic Therapy: Mechanisms of Their Generation and Potentiation. In *Advances in Inorganic Chemistry*; van Eldik, R., Hubbard, C.D., Eds.; Academic Press: Cambridge, MA, USA, 2017; Volume 70, pp. 343–394.
11. Bekeschus, S.; Clemen, R. Plasma, cancer, immunity. *J. Phys. D Appl. Phys.* **2022**, *55*, 473003. [[CrossRef](#)]
12. Chang, J.W.; Kang, S.U.; Shin, Y.S.; Kim, K.I.; Seo, S.J.; Yang, S.S.; Lee, J.-S.; Moon, E.; Baek, S.J.; Lee, K.; et al. Non-thermal atmospheric pressure plasma induces apoptosis in oral cavity squamous cell carcinoma: Involvement of DNA-damage-triggering sub-G1 arrest via the ATM/p53 pathway. *Arch. Biochem. Biophys.* **2014**, *545*, 133–140. [[CrossRef](#)] [[PubMed](#)]
13. Chang, J.W.; Kang, S.U.; Shin, Y.S.; Seo, S.J.; Kim, Y.S.; Yang, S.S.; Lee, J.-S.; Moon, E.; Lee, K.; Kim, C.-H. Combination of NTP with cetuximab inhibited invasion/migration of cetuximab-resistant OSCC cells: Involvement of NF-κB signaling. *Sci. Rep.* **2015**, *5*, 18208. [[CrossRef](#)] [[PubMed](#)]
14. Chauvin, J.; Judée, F.; Merbahi, N.; Vicendo, P. Effects of Plasma Activated Medium on Head and Neck FaDu Cancerous Cells: Comparison of 3D and 2D Response. *Anti. Cancer Agents Med. Chem.* **2018**, *18*, 776–783. [[CrossRef](#)] [[PubMed](#)]
15. Bekeschus, S.; Clemen, R.; Haralambiev, L.; Niessner, F.; Grabarczyk, P.; Weltmann, K.-D.; Menz, J.; Stope, M.; von Woedtke, T.; Gandhirajan, R.; et al. The Plasma-Induced Leukemia Cell Death is Dictated by the ROS Chemistry and the HO-1/CXCL8 Axis. *IEEE Trans. Radiat. Plasma Med. Sci.* **2020**, *5*, 398–411. [[CrossRef](#)]
16. Bundscherer, L.; Wende, K.; Ottmüller, K.; Barton, A.; Schmidt, A.; Bekeschus, S.; Hasse, S.; Weltmann, K.-D.; Masur, K.; Lindequist, U. Impact of non-thermal plasma treatment on MAPK signaling pathways of human immune cell lines. *Immunobiology* **2013**, *218*, 1248–1255. [[CrossRef](#)]
17. Bekeschus, S.; Wende, K.; Hefny, M.M.; Rödder, K.; Jablonowski, H.; Schmidt, A.; von Woedtke, T.; Weltmann, K.-D.; Benedikt, J. Oxygen atoms are critical in rendering THP-1 leukaemia cells susceptible to cold physical plasma-induced apoptosis. *Sci. Rep.* **2017**, *7*, 2791. [[CrossRef](#)]
18. Bekeschus, S.; Ressel, V.; Freund, E.; Gelbrich, N.; Mustea, A.; Stope, M.B. Gas Plasma-Treated Prostate Cancer Cells Augment Myeloid Cell Activity and Cytotoxicity. *Antioxidants* **2020**, *9*, 323. [[CrossRef](#)]
19. Hua, D.; Cai, D.; Ning, M.; Yu, L.; Zhang, Z.; Han, P.; Dai, X. Cold atmospheric plasma selectively induces G<sub>0</sub>/G<sub>1</sub> cell cycle arrest and apoptosis in AR-independent prostate cancer cells. *J. Cancer* **2021**, *12*, 5977–5986. [[CrossRef](#)]
20. Hirst, A.M.; Simms, M.S.; Mann, V.M.; Maitland, N.; O’Connell, D.; Frame, F.M. Low-temperature plasma treatment induces DNA damage leading to necrotic cell death in primary prostate epithelial cells. *Br. J. Cancer* **2015**, *112*, 1536–1545. [[CrossRef](#)]
21. Prodromidou, A.; Pandraklakis, A.; Iavazzo, C. The Emerging Role of Neutral Argon Plasma (PlasmaJet) in the Treatment of Advanced Stage Ovarian Cancer: A Systematic Review. *Surg. Innov.* **2020**, *27*, 299–306. [[CrossRef](#)]
22. Koensgen, D.; Besic, I.; Gumbel, D.; Kaul, A.; Weiss, M.; Diesing, K.; Kramer, A.; Bekeschus, S.; Mustea, A.; Stope, M.B. Cold Atmospheric Plasma (CAP) and CAP-Stimulated Cell Culture Media Suppress Ovarian Cancer Cell Growth—A Putative Treatment Option in Ovarian Cancer Therapy. *Anticancer Res.* **2017**, *37*, 6739–6744. [[CrossRef](#)] [[PubMed](#)]
23. Bisag, A.; Bucci, C.; Coluccelli, S.; Girolimetti, G.; Laurita, R.; De Iaco, P.; Perrone, A.M.; Gherardi, M.; Marchio, L.; Porcelli, A.M.; et al. Plasma-activated Ringer’s Lactate Solution Displays a Selective Cytotoxic Effect on Ovarian Cancer Cells. *Cancers* **2020**, *12*, 476. [[CrossRef](#)] [[PubMed](#)]
24. Lheureux, S.; Gourley, C.; Vergote, I.; Oza, A.M. Epithelial ovarian cancer. *Lancet* **2019**, *393*, 1240–1253. [[CrossRef](#)] [[PubMed](#)]
25. Wang, X.; Deavers, M.; Patenia, R.; Bassett, R.L.; Mueller, P.; Ma, Q.; Wang, E.; Freedman, R.S. Monocyte/macrophage and T-cell infiltrates in peritoneum of patients with ovarian cancer or benign pelvic disease. *J. Transl. Med.* **2006**, *4*, 30. [[CrossRef](#)] [[PubMed](#)]
26. Kawamura, K.; Komohara, Y.; Takaishi, K.; Katabuchi, H.; Takeya, M. Detection of M2 macrophages and colony-stimulating factor 1 expression in serous and mucinous ovarian epithelial tumors. *Pathol. Int.* **2009**, *59*, 300–305. [[CrossRef](#)] [[PubMed](#)]

27. Zhu, J.; Zhi, Q.; Zhou, B.P.; Tao, M.; Liu, J.; Li, W. The Role of Tumor Associated Macrophages in the Tumor Microenvironment: Mechanism and Functions. *Anti. Cancer Agents Med. Chem.* **2016**, *16*, 1133–1141. [[CrossRef](#)]
28. Wang, X.; Zhao, X.; Wang, K.; Wu, L.; Duan, T. Interaction of monocytes/macrophages with ovarian cancer cells promotes angiogenesis *in vitro*. *Cancer Sci.* **2013**, *104*, 516–523. [[CrossRef](#)]
29. Sica, A.; Schioppa, T.; Mantovani, A.; Allavena, P. Tumour-associated macrophages are a distinct M2 polarised population promoting tumour progression: Potential targets of anti-cancer therapy. *Eur. J. Cancer* **2006**, *42*, 717–727. [[CrossRef](#)]
30. Bekeschus, S.; Schmidt, A.; Niessner, F.; Gerling, T.; Weltmann, K.-D.; Wende, K. Basic Research in Plasma Medicine—A Throughput Approach from Liquids to Cells. *J. Vis. Exp.* **2017**, e56331. [[CrossRef](#)]
31. Reuter, S.; von Woedtke, T.; Weltmann, K.-D. The kINPen—A review on physics and chemistry of the atmospheric pressure plasma jet and its applications. *J. Phys. D Appl. Phys.* **2018**, *51*, 233001. [[CrossRef](#)]
32. Wende, K.; Reuter, S.; von Woedtke, T.; Weltmann, K.-D.; Masur, K. Redox-Based Assay for Assessment of Biological Impact of Plasma Treatment. *Plasma Process. Polym.* **2014**, *11*, 655–663. [[CrossRef](#)]
33. Candeias, L.P.; MacFarlane, D.P.S.; McWhinnie, S.L.W.; Maidwell, N.L.; Roeschlaub, C.A.; Sammes, P.G.; Whittlesey, R. The catalysed NADH reduction of resazurin to resorufin. *J. Chem. Soc. Perkin Trans.* **1998**, *2*, 2333–2334. [[CrossRef](#)]
34. Bekeschus, S.; Kolata, J.; Winterbourn, C.; Kramer, A.; Turner, R.; Weltmann, K.D.; Bröker, B.; Masur, K. Hydrogen peroxide: A central player in physical plasma-induced oxidative stress in human blood cells. *Free. Radic. Res.* **2014**, *48*, 542–549. [[CrossRef](#)] [[PubMed](#)]
35. Clemen, R.; Arlt, K.; von Woedtke, T.; Bekeschus, S. Gas Plasma Protein Oxidation Increases Immunogenicity and Human Antigen-Presenting Cell Maturation and Activation. *Vaccines* **2022**, *10*, 1814. [[CrossRef](#)]
36. Graves, D.B. The emerging role of reactive oxygen and nitrogen species in redox biology and some implications for plasma applications to medicine and biology. *J. Phys. D Appl. Phys.* **2012**, *45*, 263001. [[CrossRef](#)]
37. Privat-Maldonado, A.; Schmidt, A.; Lin, A.; Weltmann, K.-D.; Wende, K.; Bogaerts, A.; Bekeschus, S. ROS from Physical Plasmas: Redox Chemistry for Biomedical Therapy. *Oxid. Med. Cell. Longev.* **2019**, *2019*, 9062098. [[CrossRef](#)]
38. Stope, M.B.; Klinkmann, G.; Diesing, K.; Koensgen, D.; Burchardt, M.; Mustea, A. Heat Shock Protein HSP27 Secretion by Ovarian Cancer Cells Is Linked to Intracellular Expression Levels, Occurs Independently of the Endoplasmic Reticulum Pathway and HSP27's Phosphorylation Status, and Is Mediated by Exosome Liberation. *Dis. Markers* **2017**, *2017*, 1575374. [[CrossRef](#)]
39. Zhao, M.; Ding, J.X.; Zeng, K.; Zhao, J.; Shen, F.; Yin, Y.X.; Chen, Q. Heat shock protein 27: A potential biomarker of peritoneal metastasis in epithelial ovarian cancer? *Tumor Biol.* **2013**, *35*, 1051–1056. [[CrossRef](#)]
40. Khabipov, A.; Käding, A.; Liedtke, K.R.; Freund, E.; Partecke, L.-I.; Bekeschus, S. RAW 264.7 Macrophage Polarization by Pancreatic Cancer Cells—A Model for Studying Tumour-promoting Macrophages. *Anticancer. Res.* **2019**, *39*, 2871–2882. [[CrossRef](#)]
41. Arrigo, A.-P.; Firdaus, W.J.; Mellier, G.; Moulin, M.; Paul, C.; Diaz-Latoud, C.; Kretz-Remy, C. Cytotoxic effects induced by oxidative stress in cultured mammalian cells and protection provided by Hsp27 expression. *Methods* **2005**, *35*, 126–138. [[CrossRef](#)]
42. Haleabc, L.P.; Greer, P.K.; Sempowski, G.D.D. Bromelain Treatment Alters Leukocyte Expression of Cell Surface Molecules Involved in Cellular Adhesion and Activation. *Clin. Immunol.* **2002**, *104*, 183–190. [[CrossRef](#)]
43. Yoon, J.; Terada, A.; Kita, H. CD66b Regulates Adhesion and Activation of Human Eosinophils. *J. Immunol.* **2007**, *179*, 8454–8462. [[CrossRef](#)] [[PubMed](#)]
44. Prieto, J.; Eklund, A.; Patarroyo, M. Regulated Expression of Integrins and Other Adhesion Molecules during Differentiation of Monocytes into Macrophages. *Cell. Immunol.* **1994**, *156*, 191–211. [[CrossRef](#)]
45. Sade-Feldman, M.; Kanterman, J.; Klieger, Y.; Ish-Shalom, E.; Olga, M.; Saragovi, A.; Shtainberg, H.; Lotem, M.; Baniyash, M. Clinical Significance of Circulating CD33+CD11b+HLA-DR<sup>+</sup> Myeloid Cells in Patients with Stage IV Melanoma Treated with Ipilimumab. *Clin. Cancer Res.* **2016**, *22*, 5661–5672. [[CrossRef](#)] [[PubMed](#)]
46. Salari, S.; Seibert, T.; Chen, Y.-X.; Hu, T.; Shi, C.; Zhao, X.; Cuerrier, C.M.; Raizman, J.E.; O'Brien, E.R. Extracellular HSP27 acts as a signaling molecule to activate NF- $\kappa$ B in macrophages. *Cell Stress Chaperon* **2012**, *18*, 53–63. [[CrossRef](#)]